SC 1004-A (3-55)

[redacted] UNCLASSIFIED

[redacted]

# Technical Memorandum

[redacted]

SANDIA SYSTEMATIC DECLASSIFICATION REVIEW
1st Review Date: 4-15-97
Authority: EO-DOE
Name: W Layne
2nd Review Date: 4/15/97
Authority: ADD
Name: R B Craner

Classified Information
OK for Openness

SC-TM-69-57-51

PRELIMINARY INVESTIGATION OF FLAME CONFIGURATIONS
FORMED BY SONIC AND SUBSONIC HYDROGEN JETS

by

J. R. Banister, 5112-1

SANDIA SYSTEMATIC DECLASSIFICATION REVIEW
DOWNGRADING OR DECLASSIFICATION STAMP
CLASSIFICATION CHANGED TO: U
Emelda Selph 4/21/97
PERSON CHANGING MARKING DATE: 5/5/97
Carmela M Gallegos
PERSON VERIFYING MARKING & DATE
AUTHORITY: R.B. Craner
RECORD ID: 97SN1314
DATED: 4/15/97

INVENTORIED
MAY 1 0 1958
BY ORG. 2747

ABSTRACT

A small-scale study has been conducted to obtain a qualitative understanding of flame configurations formed by hydrogen jets. Results suggest scaling procedures applicable to the LASL nuclear rocket motor tests. Refinements and extensions of the small-scale test are proposed.

[redacted]

[redacted]

Case No. 407.14

January 15, 1957

UNCLASSIFIED

[redacted]

[redacted]

CENTRAL M & R
CONTROL NO. Q

66531

[redacted]

UNCLASSIFIED

[redacted]

DISTRIBUTION:

1/13A - G. A. Fowler, 5000
2/13A - M. L. Merritt, 5110
3/13A - T. B. Cook, Jr., 5111
4/13A - J. D. Shreve, Jr., 5112
For: J. R. Banister
5/13A - Margaret Edlund, UCRL
For: Hayden Gordon, Livermore
6/13A - R. E. Schreiber, LASL
7/13A - R. K. Smeltzer, 7221-3A
8-13/13A - A. D. Pepmueller, 7225

UNCLASSIFIED

[redacted]

Experimentation was necessary to establish correctness of this model as well as to ascertain, assuming the model to be correct, the number of nozzle diameters downstream to the mass mixing phase. In addition, the diameter and length of the flame as a function of nozzle diameter and conditions were studied.

A crude experiment was set up to examine the approximate variation of flame configuration from a hydrogen jet as a function of stagnation pressure, density, and nozzle diameter. This preliminary study was intended to provide an immediate tentative answer to the testing problem as well as to examine feasibility and value of further model studies.

Experimental Equipment

Figure 1 depicts experimental arrangements. Hydrogen passes through control valves out past the heater to the exit nozzle. Nitrogen was provided for rinsing the system before and after runs. To obtain higher exit velocities the heater was employed in the flow system forward of the upward-directed exit nozzle. Stagnation pressure ahead of the nozzle was determined by a head probe situated above the heater. This pressure was communicated to a Heise gage on the control board. Heater power was monitored by means of a voltmeter and an ammeter also located on the control board. Power input was controlled by a variac. An unsuccessful feature of the system was a salt-water injector installed at the controls. It was hoped that the injector would render the flame luminous by forming small salt particles through spray evaporation. Apparently, however, most of the salt particles were deposited in the line to the nozzle, and only a small amount of flame coloration was achieved.

Ignition of the hydrogen jet was achieved by using electrically heated wires. The wires were attached to a terminal board in such a manner that ignition could be attempted at various heights above the nozzle. The entire board could be moved up and down, as well as in and out, from the nozzle.

Ignition Results

Igniting the hydrogen jet proved simple. V-shaped nichrome wires were situated with the point in line with the nozzle edge. The heater wires were overvoltaged so that, after ignition,

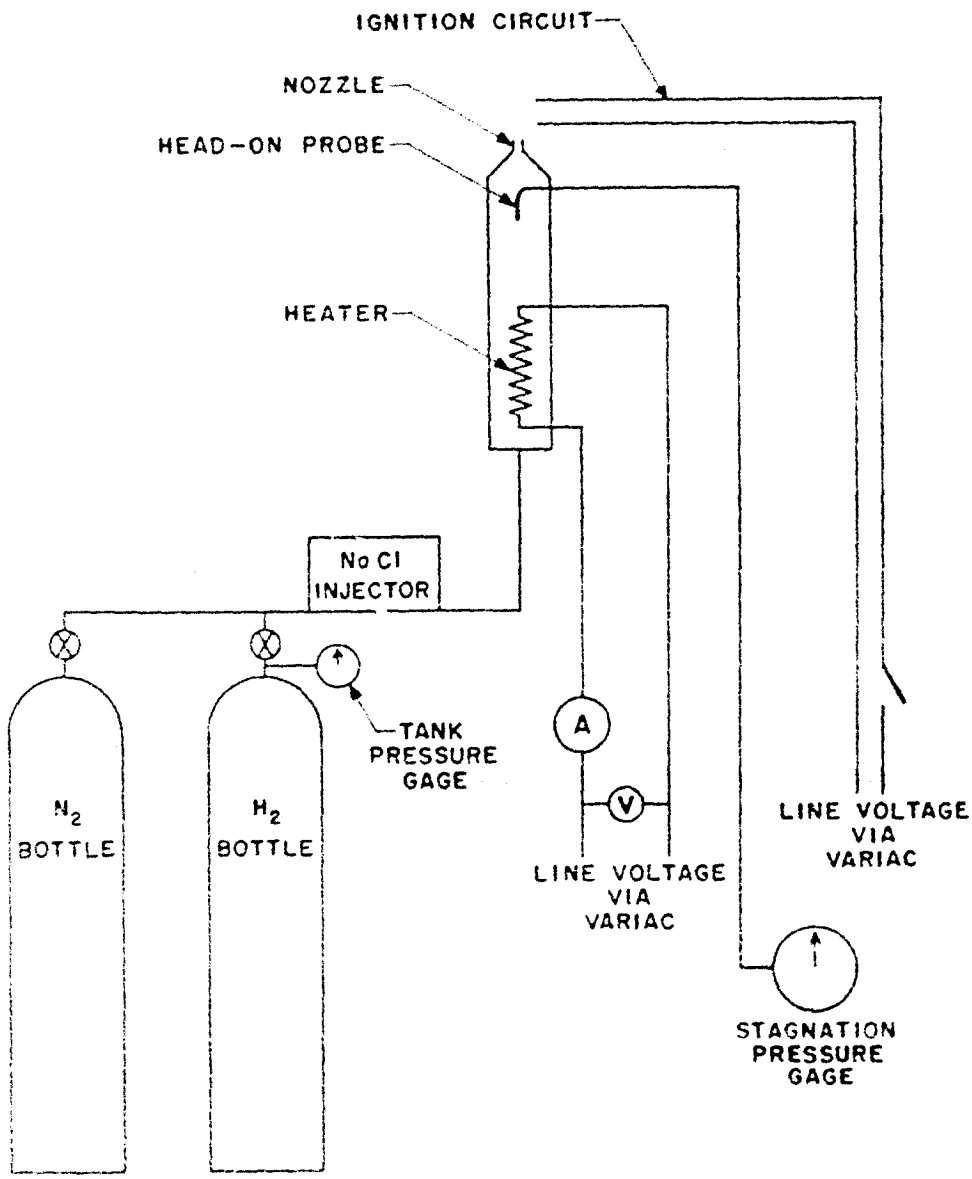


FIG. 1 - SCHEMATIC OF EXPERIMENTAL ARRANGEMENT

they melted and fell out of the flame, thus avoiding the possibility of their acting as flame holders. The hydrogen flame was not visible in daylight, although achievement of ignition was apparent from the roaring of the flame.

Ignitions were accomplished from 1/8 to 6 inches above both 1/8- and 1/16-inch nozzles, using excess chamber pressures of 12, 6, and 3 psi. However, when using the 1/16-inch nozzle and an excess chamber pressure of 18 psi, difficulty was encountered in achieving a stable flame. Although the hot wire ignited the jet, the flame went out as soon as this wire melted and dropped. No further attempts were made to secure a stable flame.

It should be noted that while the hydrogen jet proved easy to ignite, no spontaneous ignitions occurred. Apparently, the jet temperature was in all cases below the autoignition temperature (1050°C), even though low flow rates and high heater currents were employed.

Flame Configuration and Dimensions

As mentioned in the previous section, the hydrogen flame was invisible in daylight, although distortion effects brought about by the hot burned gases were apparent. Flame characteristics were examined by photography at night. A canvas screen was mounted about the jet stand to reduce wind interference. Photographs were obtained by Mr. Dale Fastle of the Optical Measurements Division, 5216, who used two Graflex cameras equipped with remote-control solenoid shutter triggers.

Flame dimensions and run conditions are enumerated in Table I. A typical flame photograph (black and white copy of color film negative) is shown in Fig. 2. Table II contains estimated initial jet velocities and densities, and mass flow computed by two methods. Computational methods, together with sources of the obvious discrepancies, are discussed in Appendix A.

Discussion and Conclusions

Viewed in darkness, burning was observed to start abruptly some distance above the nozzle. An inner cone of unburned gas was visible in the lower portion. From initial burning it expanded slowly to achieve maximum breadth which was maintained for a considerable length up the

UNCLASSIFIED

[redacted]

Table I - RUN CONDITIONS AND FLAME DIMENSIONS

| Run No. | Excess Stagnation Pressure (psi) | Nozzle Diameter (in.) | Heater Power (cal/sec) | Length from Nozzle to Flame (in.) | Initial Flame Breadth (in.) | Length from Initial Flame to Maximum Breadth (in.) | Maximum Flame Breadth (in.) | Over-All Flame Length (in.) | Remarks |
|---|---|---|---|---|---|---|---|---|---|
| 1 | 12 | 1/16 | - | 1.4 | 0.62 | 4.7 | 1.33 | 11 | Stagnation pressure varied during run (not plotted) |
| 2 | 12 | 1/16 | 215 | 1.88 | 0.78 | 3.13 | 1.4 | 7.5 | |
| 3 | 12 | 1/16 | 405 | 1.90 | 0.68 | 2.72 | 1.36 | 7.88 | |
| 4 | 6 | 1/16 | 215 | 1.4 | 0.62 | 3.16 | 1.09 | 6.25 | |
| 5 | 6 | 1/16 | 419 | 1.36 | 0.54 | 1.36 | 1.19 | 6.8 | |
| 6 | 3 | 1/16 | 0 | 0.41 | 0.27 | 4.07 | 1.09 | 7.6 | |
| 7 | 3 | 1/16 | 419 | 0.47 | 0.31 | 4.68 | 1.13 | 7.8 | |
| 8 | 12 | 1/8 | 0 | 1.83 | 0.94 | 9.4 | 2.66 | >17.5 | |
| 9 | 6 | 1/8 | 0 | 1.33 | 0.78 | 9.4 | 2.18 | >18.4 | |
| 10 | 3 | 1/8 | 0 | 0.39 | 0.31 | 9.4 | 2.12 | 18.7 | |

UNCLASSIFIED

[redacted]

UNCLASSIFIED

Table II - COMPUTED NOZZLE EXIT CONDITIONS

| Run No. | Excess Stagnation Pressure (psi) | Nozzle Diameter (in.) | Heater Power (cal/sec) | Computed from Laval Equation: Mass Flow (gm/sec) | Exit Density (gm/cm$^3$) | Exit Velocity (fps) | Mass Flow from Tank Pressure Change (gm/sec) |
|---|---|---|---|---|---|---|---|
| 1 | 12 | 1/16 | 0 | 0.254 | $0.835 \times 10^{-4}$ | 5,050 | - |
| 2 | 12 | 1/16 | 215 | 0.167 | $0.356 \times 10^{-4}$ | 7,750 | 0.21 |
| 3 | 12 | 1/16 | 405 | 0.121 | $0.192 \times 10^{-4}$ | 10,400 | - |
| 4 | 6 | 1/16 | 215 | 0.156 | $0.329 \times 10^{-4}$ | 7,860 | 0.16 |
| 5 | 6 | 1/16 | 419 | 0.0668 | $0.100 \times 10^{-4}$ | 11,000 | 0.11 |
| 6 | 3 | 1/16 | 0 | 0.129 | $0.73 \times 10^{-4}$ | 2,900 | 0.16 |
| 7 | 3 | 1/16 | 419 | 0.0358 | $0.065 \times 10^{-4}$ | 8,850 | 0.061 |
| 8 | 12 | 1/8 | 0 | 1.015 | $0.835 \times 10^{-4}$ | 5,050 | 0.92 |
| 9 | 6 | 1/8 | 0 | 0.725 | $0.767 \times 10^{-4}$ | 3,900 | 0.44 |
| 10 | 3 | 1/8 | 0 | 0.516 | $0.730 \times 10^{-4}$ | 2,900 | 0.38 |

UNCLASSIFIED

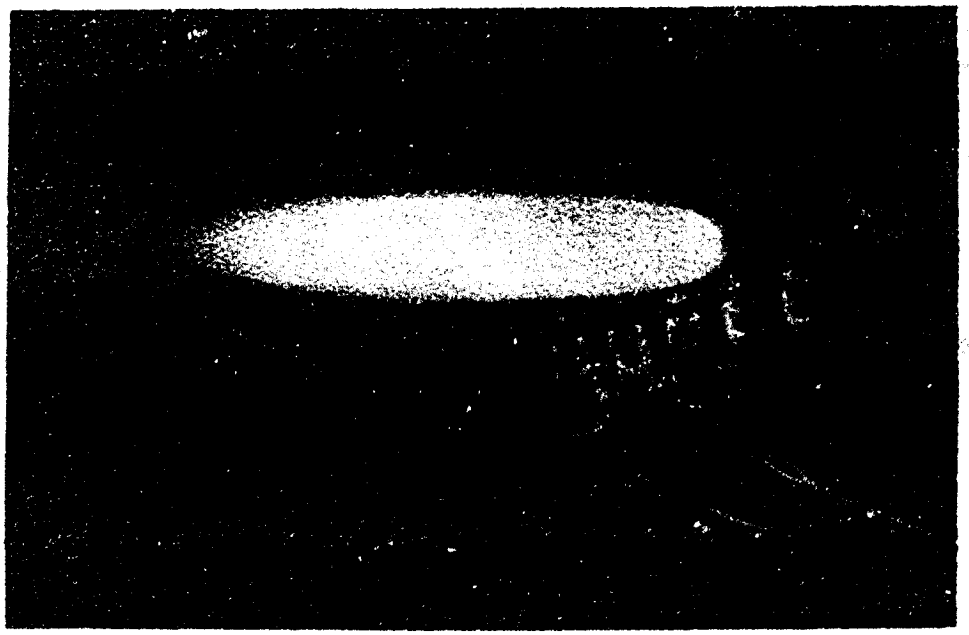

Fig. 2 - A Typical Flame

flame. It then pulled into complete the visible limit in an indistinct fashion. At low stagnation pressures the shape was markedly necked down to the base of the flame. The lower portions of the flame were light blue while the upper showed tinges of orange. This flame configuration proved very stable. Viewed from a few feet away, no flicker or movement was apparent. No attempt was made to measure the flame temperature; it was apparent, however, that its maximum was in excess of 1350°C, since extraneously placed nichrome heater wires melted in the flame.

Distances from nozzle to lower flame edge, as well as initial and maximum flame breadths, are plotted in Fig. 3. Distances to the maximum flame breadth are plotted in Fig. 4. Several interesting trends are revealed here. Flame geometry is chiefly dependent on excess stagnation pressure, since it is apparent that it is only weakly, if at all, dependent upon exit velocity or temperature, per se. In addition, the distance to the flame from the orifice does not scale with nozzle diameter, but seems to be independent of it. The same appears true of the initial flame breadth, especially if the difference in nozzle diameters is taken into account. Finally,

UNCLASSIFIED

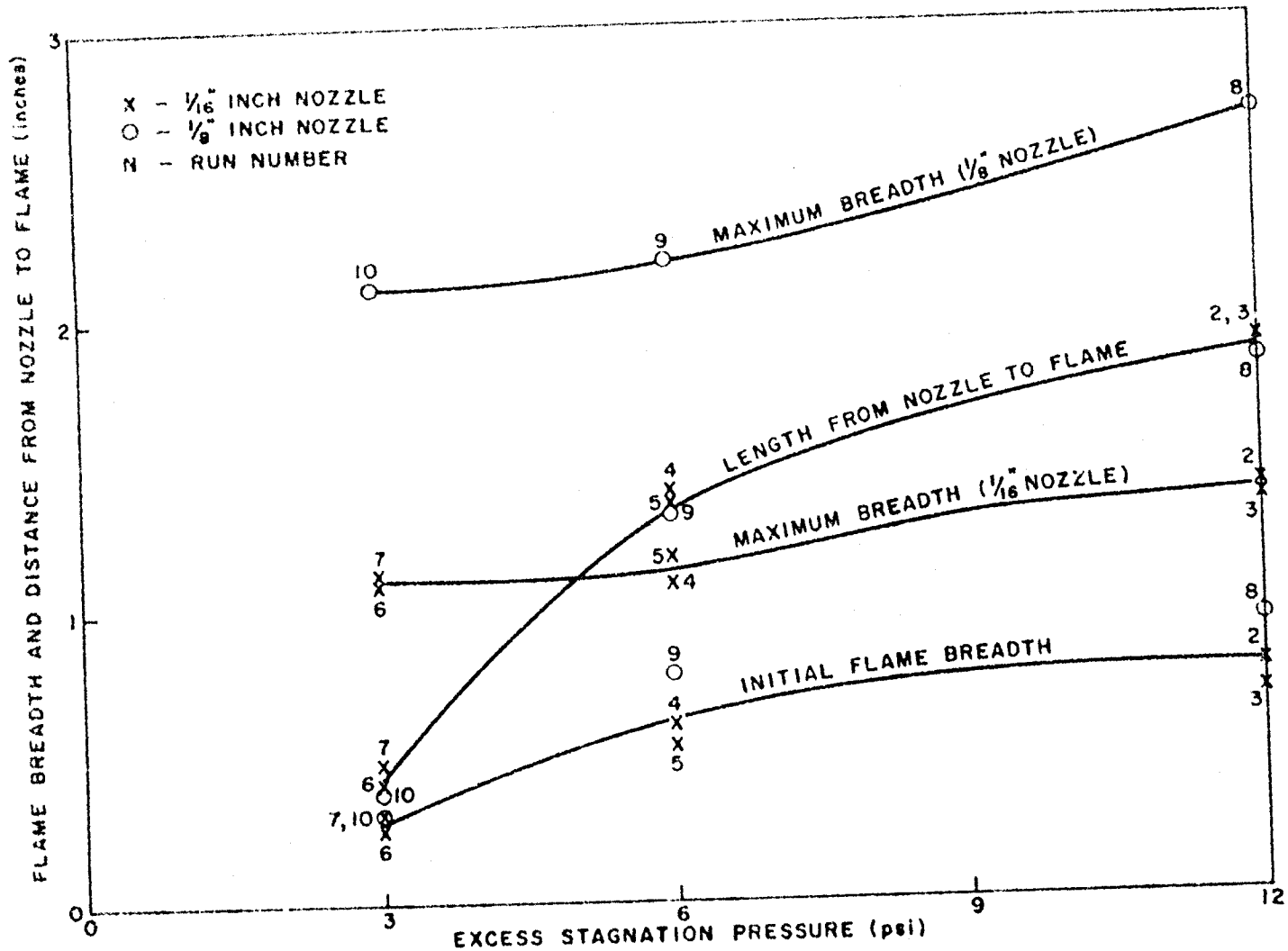


FIG. 3 – PLOT OF VARIOUS FLAME DIMENSIONS VS EXCESS STAGNATION PRESSURE

UNCLASSIFIED

UNCLASSIFIED

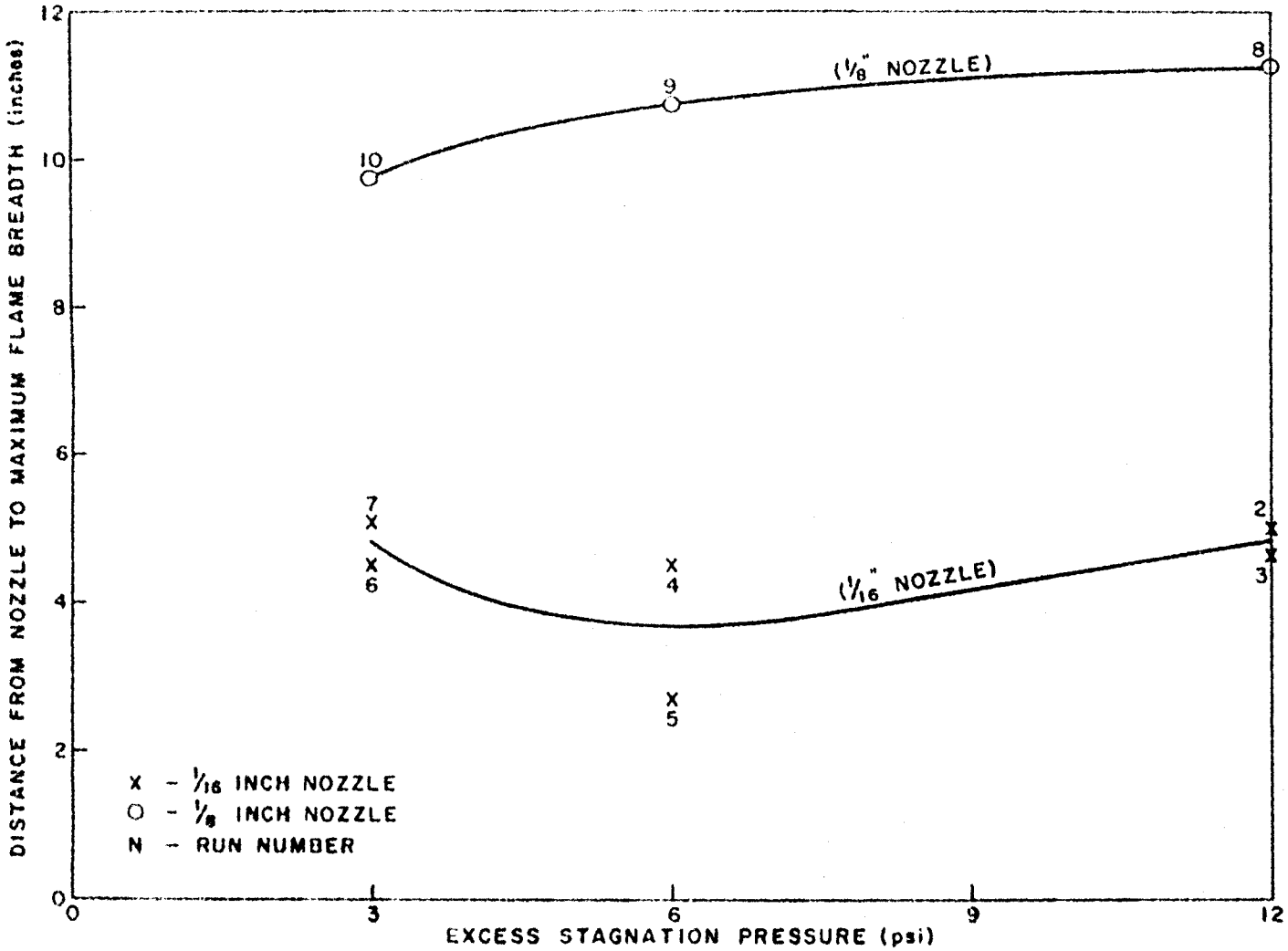


FIG. 4 - PLOT OF LENGTH TO MAXIMUM FLAME BREADTH VS. EXCESS STAGNATION PRESSURE

FILED

the maximum diameter and its distance to the nozzle scales with orifice diameter within the limits of this experiment; they also show a weak dependence on excess chamber pressure. Distance from the nozzle to the fuzzy flame termination has not been plotted. From Table II it is apparent that this quantity does not scale directly with nozzle diameter. Observation of these trends, as shown in Figs. 3 and 4, together with flame photographs, suggests that the outer flame boundary is much the same regardless of stagnation pressure, temperature, and, to a certain extent, orifice diameter. This is significant in that it indicates that the full-scale test may be expected to display a cone-shaped flame rather than one suggested by visible behavior of chemical rocket exhaust.

Other studies of subsonic jets dealing with velocity concentrations, etc., have yielded results similar to those of this experiment.[2/] While supersonic exhaust is undoubtedly a complication, mixing along the outer surface is still to be expected; it is this mixing and slowing action that determines the lower flame boundary and geometry. The range of the present experiment is too limited to permit wide claims. However, by assuming that the mixing of the supersonic jet is similar, although not identical, to that of the subsonic jet, approximate full-scale behavior may be predicted as follows:

1. The distance of the flame boundary above the nozzle will not scale with diameter, but will prove a weak function of exit jet dynamic pressure.

2. The breadth of the lower edge of the flame will be that of the nozzle plus a matter of inches.

3. While no firm basis exists for estimating the flame configuration during the supersonic phase, the flame can be expected to expand into a cone after the jet becomes subsonic. The total cone angle will probably be somewhat less than that observed in this study (13-15 degrees).[2/]

4. Expansion into a cone will continue until a maximum breadth is achieved; the maximum breadth will scale approximately with orifice diameter and show a weak dependence on mass flux and/or dynamic pressure at the nozzle exit.

5. Detailed behavior of the flame beyond maximum breadth has not be determined. Qualitatively, it would be expected to form a cylinder for some length and finally close on itself at a height which cannot be assigned from this study.

6. Ignition of the full-scale hydrogen flame should prove simple. A pilot flame or hot wire situated a diameter or more above the nozzle lip should suffice. Once ignition is achieved, the flame should maintain itself.

Future Work

The work described herein is preliminary; a clean-up phase is needed to refine results and remove the objectionable features discussed in the appendix. At the same time the experiment should be expanded to include a wider range of nozzle sizes, fuels (ammonia as well as hydrogen), and stagnation conditions.

Prior to performing an expanded experiment, however, assurance of the results of model studies scaling are needed. Theory and other experiments suggest that approximate scaling is possible.[2/]

Case No. 407.14
January 15, 1957

J. R. BANISTER - 5112-1

## APPENDIX A

In Table II there are discrepancies between mass flow rates as determined by changes of tank pressure and those computed from theory. These discrepancies, as well as the theoretical basis for the computations, are considered in the following paragraphs.

The method of computing the mass flow rate from tank pressure changes is straightforward. The perfect gas law is used to compute the mass of gas used during the timed run.

Equally straightforward is the method of computing mass flux from stagnation conditions forward of the nozzle.[3/] The Laval nozzle equation is used:

$$M = A\sqrt{\frac{2\gamma}{\gamma-1} P_o \rho_o \left(\frac{P}{P_o}\right)^{\frac{2}{\gamma}} \left(1 - \left(\frac{P}{P_o}\right)^{\frac{\gamma-1}{\gamma}}\right)} \quad . \qquad (A.1)$$

Here M is the mass flow rate, A is the nozzle area, $\gamma$ is the ratio of specific heat capacitors, $P_o$ is stagnation pressure, $\rho_o$ is stagnation density, and P is ambient pressure. This equation is valid only to values of

$$\frac{P}{P_o} > \left(\frac{2}{\gamma+1}\right)^{\frac{\gamma}{\gamma-1}} \quad .$$

For lesser values of $P/P_o$ the mass flow is constant for given stagnation conditions because of acoustic restriction.

In this experiment stagnation pressure was measured; stagnation temperature and density were not. If no heater power is supplied, stagnation temperature is ambient (291°K). If it is assumed that all of the power supplied to the heater appears in heating of the gas stream, the stagnation temperature may be computed by a comparison with an equivalent no power condition, using the equation

$$K_1 = \frac{-\frac{H}{C_p} + \sqrt{\frac{H^2}{C_p^2} + 4\,T_o^2\,M_o^2}}{2\,T_o} \quad . \qquad (A.2)$$

Here, $M_1$ is the mass flow at the elevated temperature, H is heater power supplied, $C_p$ is the specific heat at constant pressure, $T_o$ is the ambient temperature, and $M_o$ is the mass flow rate at ambient temperature. Equation A.2 may be derived using Eq A.1 along with the perfect gas law and the energy conservation equation

$$\Delta T C_p M_1 = H \quad , \tag{A.3}$$

where $\Delta T$ is temperature rise above ambient. Exit velocities, temperature, etc., may be computed by assuming the flow to be isentropic. The procedure is described in all standard texts.

The discrepancies of Table II arise from three sources: experimental errors, heat losses from the gas stream which invalidate, for lower flow rates, the use of Eqs A.2 and A.3, and the fact that the nozzles were designed for constructional expedience rather than for perfect performance. This last factor is particularly evident in the 1/8-inch nozzle results. This indicates that the proper value of A in Eq A.1 is not known, since a venturi constriction is formed which limits the effective nozzle area to less than that of the physical opening. These error sources can be reduced by using better nozzles and heat insulation. Since some heat loss is inevitable, it is advisable to use tank pressure changes as an index of mass flow rates and effective exit temperatures.

[redacted]

UNCLASSIFIED [redacted]

REFERENCES


1. Hudson, C. C., An Estimate of Thermal Flux from the Jet of a Proposed Nuclear Rocket Engine, Sandia Corporation TM-277-56-51, August 30, 1956.

2. Pai, S., Fluid Dynamics of Jets, Van Nostrand Company, New York, July 1954.

3. Liepmann, H. W. and Puckett, A. E., Aerodynamics of a Compressible Fluid, John Wiley and Sons, Inc., New York, January 1947.


UNCLASSIFIED

[redacted]